



## Adsorption of phenol onto garlic peel: optimization, kinetics, isotherm, and thermodynamic studies

P. Muthamilselvi<sup>a,\*</sup>, R. Karthikeyan<sup>b</sup>, B.S.M. Kumar<sup>a</sup>

<sup>a</sup>Department of Chemical Engineering, SRM University, Chennai, Tamilnadu, India, Tel. +91 94861 48168;  
email: muthamilselviponnuchamy@yahoo.com (P. Muthamilselvi), Tel. +91 98401 39849;

email: drrkarthi@yahoo.com (B.S.M. Kumar)

<sup>b</sup>Anjalai Ammal Mahalingam Engineering College, Kovilvenni, Tamilnadu, India, Tel. +91 04374 233749;  
email: drbsmkumar@gmail.com

Received 11 February 2014; Accepted 12 October 2014

---

### ABSTRACT

In the present study, optimization of phenol adsorption onto garlic peel (GP) was conducted with process parameters such as initial pH, adsorbent dosage, agitation speed, and contact time. The percentage removal of phenol was optimized based on these process parameters. Response surface methodology was used for optimization as it has many advantages over classical optimization methods. A Box–Behnken experimental design was employed. The optimum conditions for maximum removal of phenol from an aqueous solution of 50 mg L<sup>-1</sup> were found as follows: pH: 2, adsorbent dosage: 2.1 g L<sup>-1</sup>, contact time: 7 h, and agitation speed: 135 rpm. At these optimized conditions, batch adsorption experiments were conducted to study the effects of initial concentration and temperature on phenol removal. Thermodynamic parameters such as  $\Delta G^\circ$ ,  $\Delta H^\circ$  and  $\Delta S^\circ$  were also evaluated. From the results, the sorption process was found to be spontaneous and exothermic. The equilibrium experimental data were analyzed with several isotherm models. The adsorption kinetics for phenol removal by GP follows the pseudo-second-order kinetic model. The results from the study demonstrated that more than 80% phenol removal is possible at the above-mentioned optimum conditions.

*Keywords:* Phenol; Garlic peel; Kinetics; Equilibrium; Thermodynamics

---

### 1. Introduction

Water scarcity is a major problem worldwide and at the same time, there is increased pollution of water. Rapid population and economic growth and industrial developments have increased water usage. Wastewater contains pathogens, nutrients such as nitrogen, phosphorus, solids, chemicals from cleaners, disinfectants, and even hazardous substances. The principal

objective of wastewater treatment is to dispose of industrial effluents without any danger to human health or harm to the environment. Phenols are categorized as an extremely hazardous pollutant since they are harmful at low concentration levels [1–3]. Over the years, adsorption has been considered to be one of the efficient methods [4,5] among various physico-chemical methods [6–9] available for the removal of phenol from aqueous effluents. Conventional adsorbents such as activated carbon [10–14] are costly;

---

\*Corresponding author.

therefore, identification of low-cost adsorbents would be greatly beneficial to the community as a whole. A number of studies have been reported in the literature in which low-cost adsorbents such as fly ash [15], rice husk char [16], pyrolyzed sewage sludge [17], lignite [18], *Sargassum muticum* [19], spent oil shale [20], bentonite [21], natural clay [22], wheat bran [23], and clay algae [24] were used as an alternative to activated carbon.

Garlic peel (GP) is abundantly available as a waste product in India. It is used as an adsorbent for the removal of methylene blue [25], as well as heavy metals including copper [26], lead [27], and nickel [28]. GP is a plant fiber that consists of cellulose, hemicellulose, and pectin substances. These species contain a large number of functional groups such as the hydroxyl, amino, and carboxyl groups [29] that bond with phenol molecules. The peel after processing does not have any unpleasant odor and is biodegradable.

Most of the adsorption studies use conventional methods by varying one factor while maintaining all other factors at constant levels. Thus, conventional optimization processes cannot identify the interaction between any two factors in a multivariable system. The response surface method—a collection of statistical and mathematical techniques—is useful for developing, improving, and optimizing processes [30–33].

Considering the abundant availability of GP and its potential as an adsorbent, experimental studies were conducted to assess its utility for removing phenol from aqueous solutions and to also carry out parametric studies with a view to optimize the conditions for maximum removal using the response surface method. Based on a review of available literature, this is the first study involving the usage of GP to remove phenol.

## 2. Materials and methods

### 2.1. Phenol stock solution

Analytical grade phenol (AR) was obtained from Southern Scientific Corporation India Chemicals Ltd., India. It was used to prepare the synthetic adsorbate solution of various initial phenol concentrations ( $C_0$ ) in the range of 50–350 mg L<sup>-1</sup>. The stock solution required was prepared every day and stored in a brown color glass reservoir of 2 L capacity to prevent photooxidation.

### 2.2. Preparation and characterization of adsorbent

GPs were collected from the student hostel of SRM university and washed with raw water to remove impurities. The peels were washed with distilled

water and dried in a hot air oven until they became crisp. The dried peels were hand crushed and then ground in a domestic mixer–grinder. The dried materials were sieved to desired mesh size (100–150  $\mu\text{m}$ ). The prepared GP sample was stored in a plastic container. No other physical or chemical treatment was used prior to the adsorption experiments. Characteristics of the GP were determined and the results are summarized in Table 1.

#### 2.2.1. FTIR study

FTIR spectra (Model: Bruker Alpha T) were obtained for the sorbents before and after phenol adsorption. Figs. 1 and 2 show the FTIR spectra of GP before and after phenol adsorption. Before adsorption, there are three noticeable peaks in the FTIR spectrum. The broad bands at 3,567 cm<sup>-1</sup> represent the –OH groups, and the peak around 1,635 cm<sup>-1</sup> corresponds to a C=O stretch. The bands observed at about 831 cm<sup>-1</sup> could be assigned to the C–H group. There is increasing transmittance with extra peaks arising from phenol molecules that have entered the structure indicating phenol adsorption by GP from the aqueous solution. The peaks at 1,373 cm<sup>-1</sup> and 776 cm<sup>-1</sup> indicate the presence of the aromatic –CH group. These observations confirm the adsorption of phenol by GP.

#### 2.2.2. SEM and EDX analysis

A scanning electron microscope equipped with energy dispersive X-ray analysis (Quanta FEG-200, FEI Netherland) was used to characterize the adsorbent. Small pieces of the sorbent samples were subjected to a 10 kV accelerating voltage. SEM micrographs of raw GP and phenol-loaded GP are shown in Fig. 3(a) and (b), respectively. Fig. 3(a) shows the presence of irregular, rough, and porous surface morphology, which indicates a high surface area of the sorbent. Fig. 3(b) clearly shows the changes on the surface of the sorbent indicating the sorption to be a surface phenomenon.

The chemical characterization of the powder before and after adsorption, as shown in Figs. 4 and 5,

Table 1  
Physical properties of GP used in the experiments

Parameters	Values
Moisture content (%)	2.69
Volatile matter (%)	68.54
Ash (%)	7.67
Fixed carbon	21.12

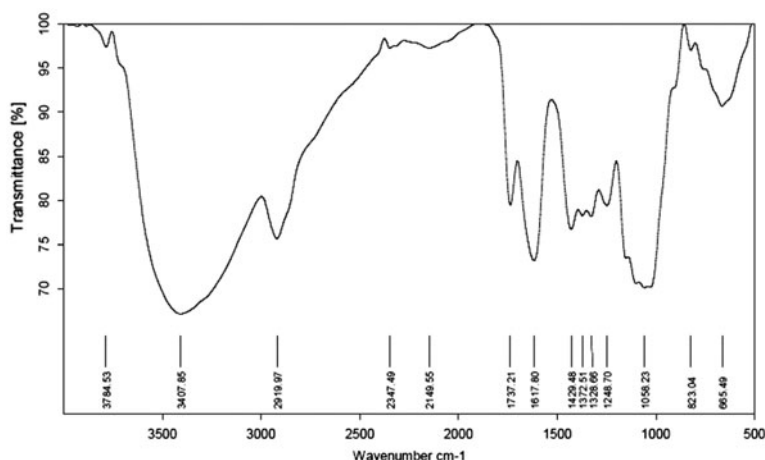


Fig. 1. FTIR spectrum of pure GP.

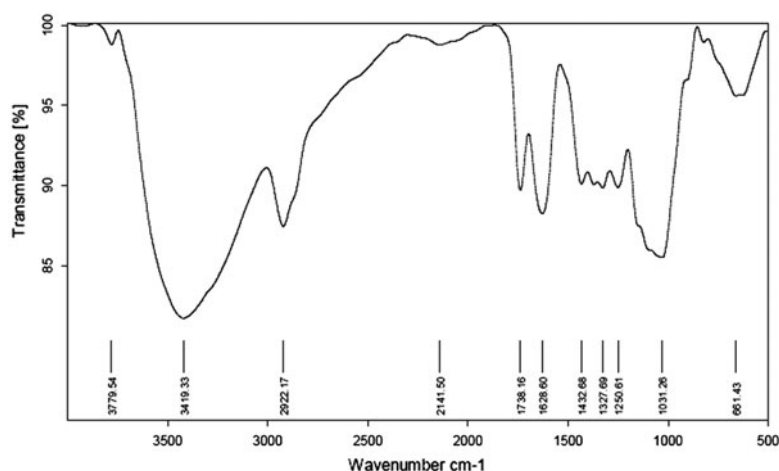


Fig. 2. FTIR spectrum of phenol-loaded GP.

Table 2  
Chemical characterization of GP before and after adsorption

	Elements				
	C	O	Ca	K	Mg
Before adsorption (%)	50.37	47.76	1.34	0.37	0.16
After adsorption (%)	50.91	47.81	1.29	–	–

changes the characteristics of the surface of the GP powder (Table 2).

### 2.2.3. Point of zero charge

Zero point charge ( $pH_{zpc}$ ) of the adsorbent was determined by the powder addition method [34]. One g of GP was added to a 100-mL conical flask

containing 50 mL of 0.1 M NaCl solution. The electrolyte solution with the GP was equilibrated for 24 h. After equilibration, the final pH ( $pH_f$ ) was recorded. Several batches were prepared with different initial solution pH ( $pH_i$ ). The pH was adjusted using 0.1 M HCl and 0.1 M NaOH solution. The change in solution pH ( $\Delta pH = pH_i - pH_f$ ) was recorded for each solution and a plot of  $\Delta pH$  vs. initial pH was prepared. The pH at which  $\Delta pH$  becomes zero is called  $pH_{zpc}$ . Fig. 6 shows the results of the experimental measurements from the  $pH_{zpc}$  study. The resulting curve intersects at a pH of around 3.9, at which the surface charge is zero. This result indicates that the  $pH_{zpc}$  of GP is about 3.9. This means that the surface of GP is positively charged in solutions with a pH below the point of zero charge and negatively charged in solutions with a pH above the point of zero charge.

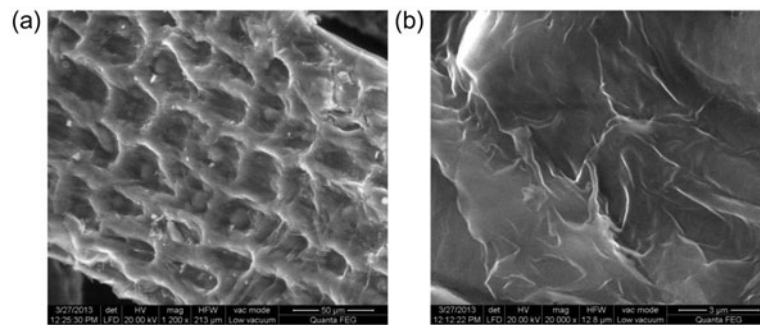


Fig. 3. Scanning electron micrograph image of (a) pure GP (b) phenol-loaded GP.

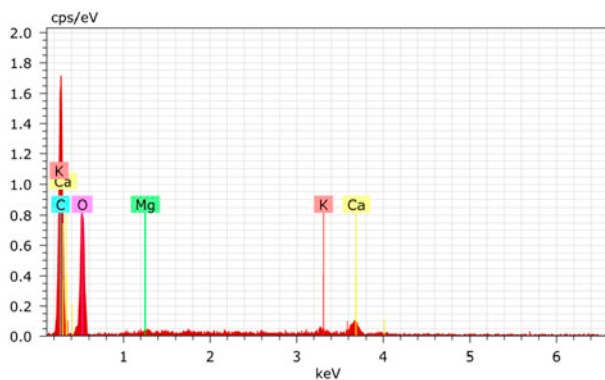


Fig. 4. Energy-dispersive X-ray spectroscopy (EDX) pure GP.

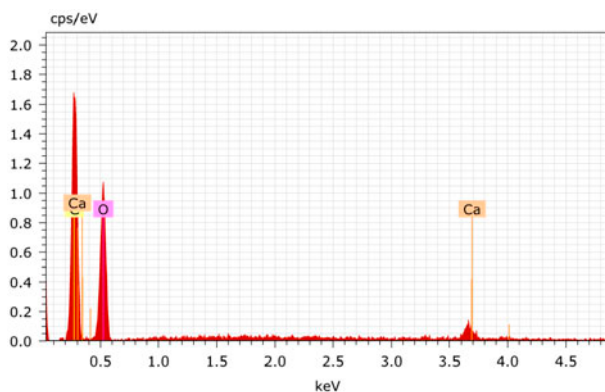


Fig. 5. EDX of phenol-loaded GP.

### 2.3. Batch adsorption studies

Adsorption experiments were conducted as per the design developed with response surface Box–Behnken methodology. The experiments were carried out in 250-mL Erlenmeyer flasks with a working volume of 100 mL of reaction mixture. The initial pH of the solution was adjusted to the desired value by adding

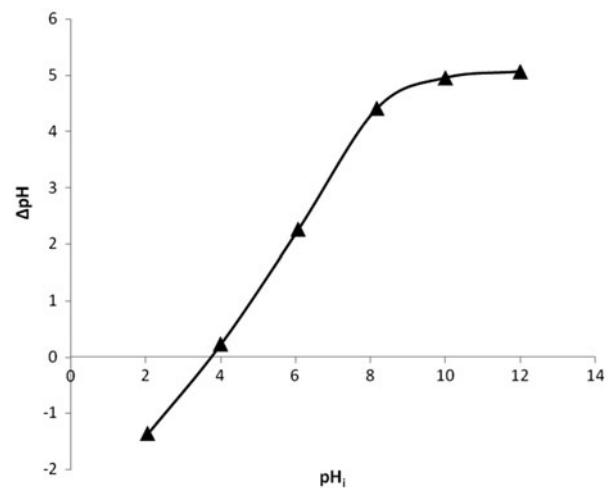


Fig. 6. Point of zero charge of GP.

0.1 M NaOH and HCl. The flasks were shaken for the specified time period in a rotary shaker and were withdrawn from the shaker after the desired time of reaction. Then, the peels were separated from the solution with Whatman filter paper No. 42. The concentration of residual phenol in the reaction mixture was measured using a spectrophotometer. Each determination was repeated three times, and the given results are the average value.

The phenol removal was taken as a response.

$$Y(\%) = \left( \frac{C_0 - C_t}{C_0} \right) 100 \quad (1)$$

where  $Y$  (%) is the percentage removal of phenol, and  $C_0$  and  $C_t$  ( $\text{mg L}^{-1}$ ) are the initial and final concentrations of phenol solutions, respectively. The process variables, pH, adsorbent dosage, contact time, and agitation speed were optimized and the effects of initial phenol concentration and temperature were studied.

Adsorption capacity of the GP was calculated using the following equation:

$$q_e = \frac{V(C_0 - C_e)}{W} \quad (2)$$

where  $q_e$  (mg g<sup>-1</sup>) is the amount of phenol adsorbed by the GP,  $C_e$  (mg L<sup>-1</sup>) is the liquid-phase concentration of phenol at equilibrium,  $V$  (L) is the volume of the solution, and  $W$  (g) is the mass of dry sorbent used.

#### 2.4. Experimental design and statistical analysis by RSM

Response surface methodology was used to determine the optimum percentage removal of phenol by garlic peel by varying different parameters such as initial solution pH, adsorbent dosage, contact time, and agitation speed. The optimization process involves three major steps, namely performing the statistically designed experiments, estimating the coefficients in a mathematical model, and predicting the response and checking the adequacy of the model. For statistical calculations, the variables  $x_i$  were coded as  $X_i$  according to the following equation:

$$X_i = \frac{x_i - x_0}{\Delta_x} \quad i = 1, 2, 3, \dots k \quad (3)$$

where  $X_i$  = coded (dimensionless) value of the variables  $x_i$ ,  $x_0$  = the value of  $x_i$  at the center point and  $\Delta_x$  = the step change.

The behavior of the system was explained by the following second-order polynomial equation:

$$Y = \beta_0 + \sum \beta_i x_i + \sum \beta_{ii} x_i^2 + \sum \beta_{ij} x_{ij} \quad (4)$$

where  $Y$  is the predicted response,  $\beta_0$  is the offset term,  $\beta_i$  is the linear effect,  $\beta_{ii}$  is the squared effect, and  $\beta_{ij}$  is the interaction effect. Parameter such as pH, adsorbent dosage, contact time, and agitation speed were chosen as the critical variables and designated as  $X_1$ ,  $X_2$ ,  $X_3$ , and  $X_4$ , respectively. The low, middle, and high levels of each variable (equally spaced) were designated 1, 0, and +1, respectively, and these levels are given in Table 3. A statistical program package, Design Expert 7.1.5, was used for regression analysis of the data obtained and to estimate the coefficient of the regression equation. The equation was validated by analysis of variance (ANOVA). The significance of each term in the equation was to estimate the goodness of fit in each case. Response surfaces were drawn

Table 3

Variables and levels considered for the adsorption of phenol using GP by Box–Behnken design

Factors	Code	Levels		
		-1	0	+1
pH	$X_1$	2	5	8
Sorbent dosage (g L <sup>-1</sup> )	$X_2$	1	2	3
Contact time (h)	$X_3$	1	4	7
Agitation speed (rpm)	$X_4$	100	125	150

to determine the individual and interactive effects of the test variables on the percentage removal of phenol. The optimal values for each test variable were first obtained in coded units and then converted to uncoded units.

### 3. Results and discussion

#### 3.1. Development of the regression model analysis

The mathematical model below relates the percentage removal to the independent process variables and gives the second-order polynomial coefficient for each term of the equation determined through multiple regression analysis using Design Expert 7.1.5:

$$\begin{aligned} \% \text{ Phenol removal} = & 70.82 - 7.16X_1 + 1.35X_2 + 3.45X_3 \\ & + 5.14X_4 - 2.10X_1X_2 - 1.53X_1X_3 \\ & + 2.40X_1X_4 - 0.98X_2X_3 \\ & - 0.025X_2X_4 + 4.50X_3X_4 - 1.39X_1^2 \\ & - 5.21X_2^2 - 4.21X_3^2 - 1.84X_4^2 \quad (5) \end{aligned}$$

The experimental and predicted values of percentage adsorption of phenol are given in Table 4. The results were analyzed by ANOVA and are given in Table 5. A quadratic regression model indicates the significance of the proposed model. The model F value of 11.52 implies that the model is considerable. In this case,  $X_1$ ,  $X_3$ ,  $X_4$ ,  $X_3X_4$ ,  $X_2^2$ ,  $X_3^2$  were significant model terms. The predicted  $R^2$  of 0.7499 reasonably agrees with the adjusted  $R^2$  of 0.8402. The fit of the model was also expressed by the coefficient of regression  $R^2$ , which was found to be 0.9201, indicating that 92.01% of the variability in the response could be explained by the model. This implies that the predicted experimental data are satisfactory. To achieve the maximum adsorption of phenol using GP, the optimum process variables were found from the developed mathematical model. The optimum conditions suggested by the model for the process variable such as pH, adsorbent

Table 4

Experimental design matrix and responses for the adsorption of phenol using GP

Run no.	$X_1$ -pH	$X_2$ -Sorbent dosage (g L <sup>-1</sup> )	$X_3$ -contact time (h)	$X_4$ -Agitation period (rpm)	% Phenol removal	
					Experimental	Theoretical
1	0	-1	-1	0	56.8	55.658
2	0	1	0	-1	61.3	58.912
3	0	0	0	0	70.8	70.867
4	0	0	-1	-1	57.4	57.496
5	0	-1	0	-1	58.6	56.946
6	0	0	1	1	80.2	75.579
7	-1	0	1	0	79.8	77.379
8	0	1	0	1	72.5	68.929
9	1	0	0	-1	50.8	52.908
10	-1	-1	0	0	64.7	69.213
11	0	1	-1	0	60.9	59.525
12	-1	0	0	1	76.9	77.842
13	0	0	0	0	70.9	70.867
14	1	0	0	1	63.7	63.775
15	0	-1	1	0	61.2	65.625
16	1	-1	0	0	59.5	56.196
17	0	1	1	0	61.4	65.592
18	0	0	0	0	70.9	70.867
19	0	-1	0	1	69.9	67.063
20	1	0	1	0	61.2	59.462
21	0	0	-1	1	59.9	61.912
22	-1	0	0	-1	73.6	68.575
23	-1	0	-1	0	69.8	66.312
24	1	0	-1	0	57.3	54.496
25	1	1	0	0	58.6	56.262
26	-1	1	0	0	72.1	72.979
27	0	0	1	-1	59.7	59.863

dosage, contact time, and agitation speed are 2, 2.1 g L<sup>-1</sup>, 7 h, and 135 rpm, respectively, with a maximum phenol removal of 82%. Similar behavior has been observed for the adsorption of phenol by various low-cost adsorbents [35–39].

### 3.2. Interaction effects of process variables

To investigate the interactive effect of two factors on the percentage removal of phenol, three-dimensional plots were drawn. Response surface plots as a function of two factors while maintaining all other factors at fixed levels are more helpful in understanding both the main and interactive effects of the two factors. The response surface curves were plotted to understand the interaction of the variables and to determine the optimum maximum response level of each variable. The response surface curves for percentage removal of phenol are shown in Fig. 7. The nature of the response surface curves shows the interaction between the variables. An elliptical shaped curve

indicates good interaction of the two variables, whereas a circular shape indicates no interaction between the variables. From this figure, it was observed that the elliptical nature of the contour in the graphs depicted the mutual interactions of all the variables.

The combined effect of pH and adsorbent dosage on percentage removal of phenol using GP is shown in Fig. 6(a). When pH exceeds 4, the removal of phenol suddenly drops. This can be attributed to the dependency of phenol ionization on the pH value and point of zero charge for GP. The point of zero charge of GP is 3.9. For pH < p<sub>HZPC</sub>, a significantly high electrostatic attraction [40–42] exists between the positively charged surface of the adsorbent and the phenolate ion (C<sub>6</sub>H<sub>5</sub>O<sup>-</sup> ion). Phenol, being a weak acid, is adsorbed to a lesser extent at higher pH values as the negatively charged surface of the adsorbent does not favor the adsorption of C<sub>6</sub>H<sub>5</sub>O<sup>-</sup> ion due to electrostatic repulsion [43–46]. This was also observed in Fig. 6(b) and (c). The percentage removal of phenol

Table 5  
ANOVA for response surface quadratic model

Source	Sum of square	Df	Mean square	F value	p > F
Model	1,478.20	14	105.59	11.52	<0.0001
X <sub>1</sub>	614.90	1	614.90	67.08	<0.0001
X <sub>2</sub>	21.87	1	21.87	2.39	0.1447
X <sub>3</sub>	142.83	1	142.83	15.58	0.0015
X <sub>4</sub>	317.24	1	317.24	34.61	<0.0001
X <sub>1</sub> X <sub>2</sub>	17.64	1	17.64	1.92	0.1871
X <sub>1</sub> X <sub>4</sub>	9.30	1	0.30	1.01	0.3309
X <sub>1</sub> X <sub>4</sub>	23.04	1	23.04	2.51	0.1352
X <sub>2</sub> X <sub>3</sub>	3.80	1	3.80	0.41	0.5300
X <sub>2</sub> X <sub>4</sub>	2.500E-003	1	2.500E-003	2.727E-004	0.9871
X <sub>3</sub> X <sub>4</sub>	81.00	1	81.00	8.84	0.0101
X <sub>1</sub> <sup>2</sup>	12.59	1	12.5	1.37	0.2607
X <sub>2</sub> <sup>2</sup>	175.79	1	175.7	19.18	0.0006
X <sub>3</sub> <sup>2</sup>	114.74	1	114.74	12.52	0.0033
X <sub>4</sub> <sup>2</sup>	22.04	1	22.04	2.40	0.1433
Residual	128.34	14	9.17		
Lack of fit	128.31	10	12.83	1,832.99	<0.0001
Pure error	0.028	4	7.000E-003		
Total	1,606.53	28			

Note:  $S = 3.03$ ,  $R^2 = 0.9201$ ,  $R^2$  (pred) = 0.7499,  $R^2$  (adj) = 0.8402.

increased with an increased adsorbent dosage. This increase in phenol removal may be due to the complete utilization of all active sites in the adsorbent dosage. This is clearly depicted in Fig. 6(a), (d), and (e).

The combined effect of pH and contact time on percentage removal of phenol using GP powder is shown in Fig. 6(b). It is observed that the removal of phenol increases to some extent with an increase in contact time. Further increase in contact time does not increase the uptake due to deposition of phenol on the available adsorption site [47]. This was also observed in Fig. 6(d) and (f).

The combined effect of pH and agitation speed on percentage removal of phenol using GP powder is shown in Fig. 6(c). The rate of agitation is an important factor for the batch removal study. From Fig. 6(c), it is evident that the percentage phenol removal increases when the agitation rate is increased to 135 rpm, beyond which there is a decline in the removal efficiency of phenol. An increase in agitation rate decreases film resistance to the mass transfer surrounding the sorbent particles, thus increasing sorption of phenol molecules [48–50]. At very high agitation speeds, there is an increase in turbulence attributable to the decrease in boundary layer thickness around the adsorbent particles, thus reducing removal efficiency [51,52].

From the data of Table 4, it is inferred that the quadratic terms of pH, adsorbent dose, contact time,

and agitation speed have a negative effect on the phenol removal percentage. Further, the interaction of contact time and agitation speed have a positive effect, whereas the interaction of pH and adsorbent dosage, pH and contact time, pH and agitation speed, adsorbent dosage and contact time, and adsorbent dosage and agitation speed have a negative effect on the phenol removal percentage. Optimum conditions for the percentage of phenol removal using GP were obtained by using RSM. Second-order polynomial models obtained in this study were utilized for each response to determine the specified optimum conditions. The optimum values obtained by substituting the respective coded values of variables are as follows: pH: 2, adsorbent dosage: 2.1 g L<sup>-1</sup>, contact time: 7 h, and agitation speed: 135 rpm. At these conditions, the maximum percentage removal was calculated. The stationary point or central point is the point at which the slope of the contour is zero in all directions. The coordinates of the central point within the highest contour levels in each of these figures will correspond to the optimum values of the respective constituents. The maximum predicted phenol removal is indicated by the surface confined in the smallest curve of the contour diagram. The optimum values drawn from these figures are in close agreement with those obtained by optimizing the regression model Eq. (5). The sequential quadratic programming in MATLAB 7 was used to solve the second-degree polynomial regression

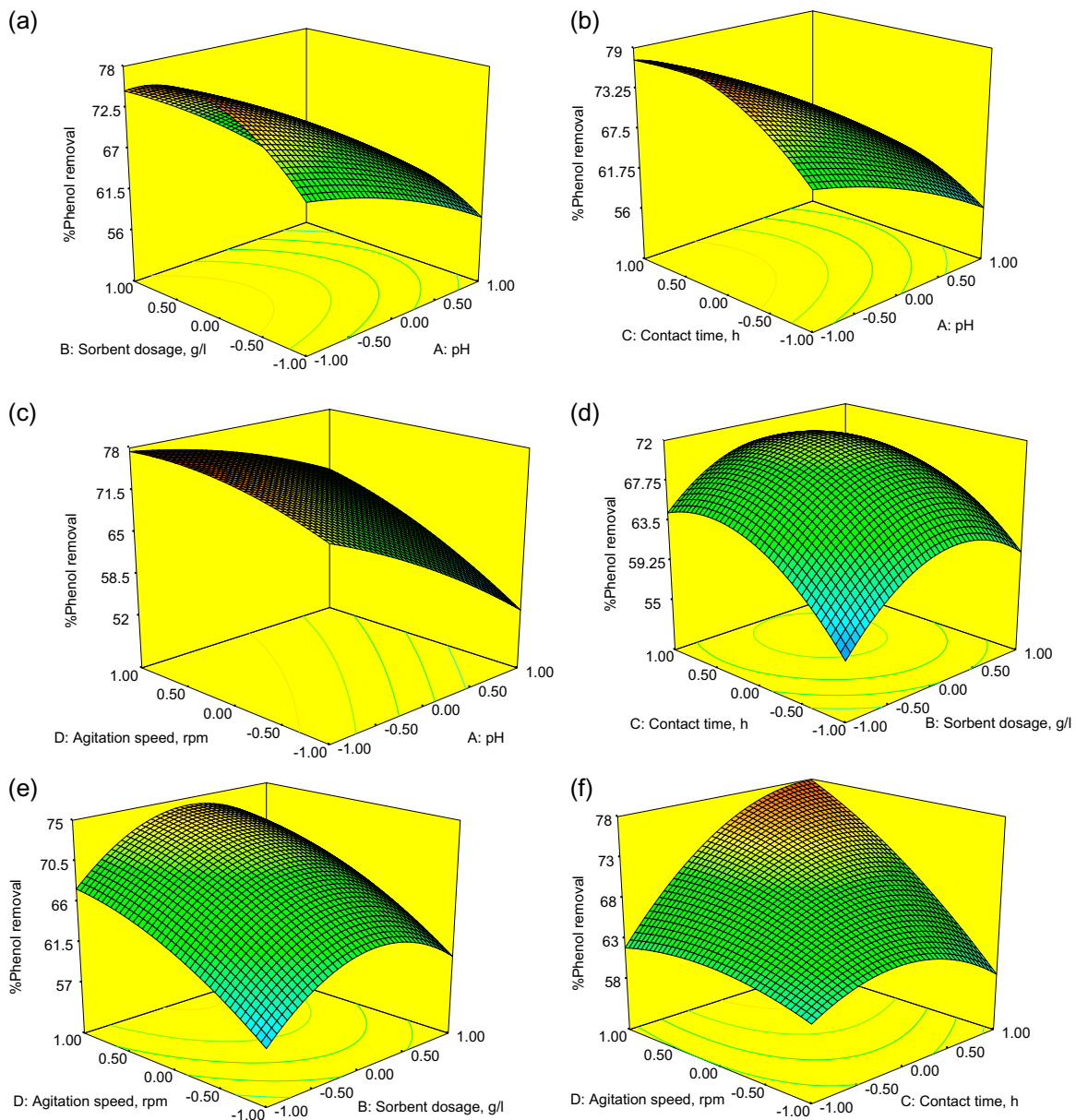


Fig. 7. 3D response surface plots: interactive effects of (a) pH and adsorbent dosage, (b) pH and contact time, (c) pH and agitation speed, (d) sorbent dosage and contact time, (e) sorbent dosage and agitation speed, and (f) contact time and agitation speed on percentage removal of phenol.

Eq. (5). The optimal values for the variables as predicted by MATLAB were found to be within the design region. This shows that the model correctly explains the influence of the chosen variables on the percentage of phenol removal.

### 3.3. Effect of initial phenol concentration

Figs. 8 and 9 show the results obtained for the effect of the initial concentration of phenol on the

removal efficiency and adsorption capacity of GP. At any time, the amount of phenol adsorbed per unit weight of adsorbent increased with an increasing concentration of phenol. The concentration provides the necessary driving force to overcome the resistance to the mass transfer of phenol between the aqueous and solid phases. The increase in concentration also enhances the interaction between phenol and GP. Therefore, an increase in concentration of phenol enhances the adsorption capacity of GP. But the

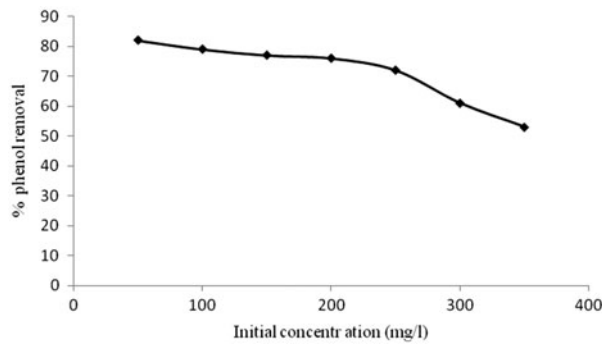


Fig. 8. Effect of initial phenol concentration on removal of phenol by GP (pH: 2; adsorbent dosage: 2.1 g L<sup>-1</sup>; contact time: 7 h; agitation speed: 135 rpm, Temp.: 30°C).

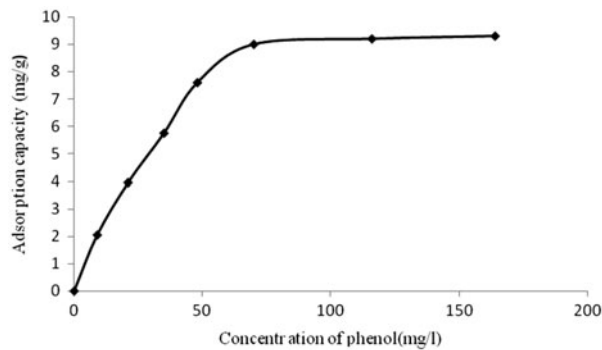


Fig. 9. Effect of concentration of phenol on the adsorption capacity (pH: 2; adsorbent dosage: 2.1 g L<sup>-1</sup>; contact time: 7 h; agitation speed: 135 rpm, Temp.: 30°C).

adsorbent shows saturation at high phenol concentration (Fig. 9) as it offers a limited number of surface binding sites. The removal efficiency of GP for removing phenol from aqueous solution remains nearly constant at low initial concentrations of phenol and decreases with an increase in initial concentrations of phenol (Fig. 8). The low removal efficiency of GP at high phenol concentration may be due to the adsorption capacity of the adsorbent attaining its maximum saturated level and therefore it no longer can increase with an increase in the concentration of phenol. This phenomenon is consistent with the trend reported in the literature [53,54].

### 3.4. Effect of temperature and thermodynamic parameters

Temperature had a pronounced effect on the adsorption capacity of adsorbents. Fig. 10 shows the experimental results obtained from phenol adsorption when temperatures were varied from 25 to 45°C. The

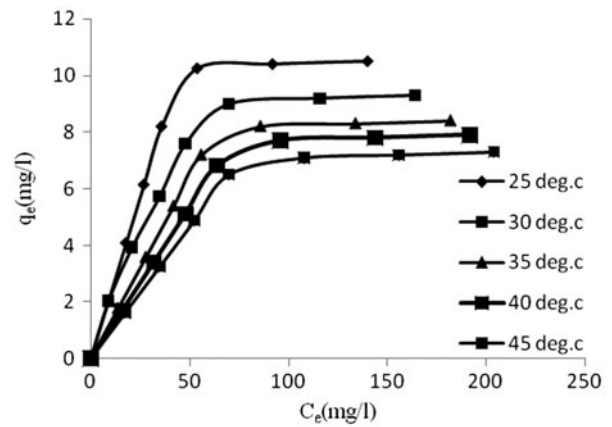


Fig. 10. Effect of temperature on phenol removal (pH: 2; adsorbent dosage: 2.1 g L<sup>-1</sup>; contact time: 7 h; agitation speed: 135 rpm).

adsorption efficiency decreased with an increase in temperature. The decrease in adsorption efficiency indicates an exothermic process. This may be due to the increasing trend to desorb phenol from the interface to the solution or the distorted active sites on the adsorbent [55]. The thermodynamic parameters that must be considered to determine the adsorption processes are the changes in standard enthalpy, standard entropy, and standard free energy due to the transfer of unit moles of solute from the solution onto the solid–liquid interface. The thermodynamic parameters  $\Delta G^\circ$ ,  $\Delta H^\circ$ , and  $\Delta S^\circ$  can be determined by using

$$\Delta G^\circ = -RT \ln b \tag{6}$$

$$\Delta G^\circ = \Delta H^\circ - T\Delta S^\circ \tag{7}$$

where  $R$  is the universal gas constant (8.314 J mol<sup>-1</sup> K),  $T$  is the temperature in Kelvin, and  $b$  known as the equilibrium constant is equal to the amount of adsorbent divided by the amount in solution.

$$-RT \ln b = \Delta H^\circ - T\Delta S^\circ \tag{8}$$

$$\ln b = \left( \frac{\Delta H^\circ}{-RT} \right) - \left( \frac{T\Delta S^\circ}{-RT} \right) \tag{9}$$

The linearized form of the above-mentioned vant Hoff's equation is given below (Fig. 11).

$$\ln b = \left( \frac{\Delta S^\circ}{R} \right) - \frac{\Delta H^\circ}{R} \left( \frac{1}{T} \right) \tag{10}$$

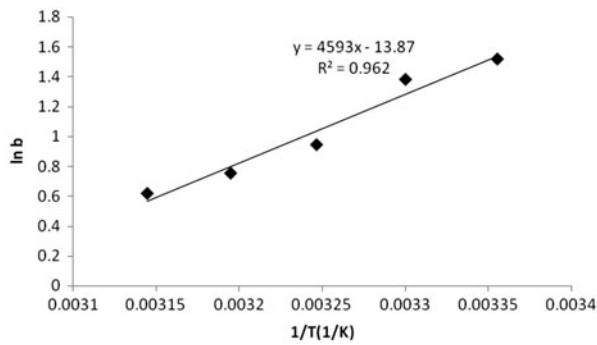


Fig. 11. Plot of  $\ln b$  vs.  $1/T$  for estimation of thermodynamic parameters for phenol adsorption onto GP.

The calculated values of Gibbs free energy ( $\Delta G^\circ$ ), enthalpy ( $\Delta H^\circ$ ), and entropy ( $\Delta S^\circ$ ) changes are given in Table 6. The negative  $\Delta G^\circ$  values indicate that the process is thermodynamically feasible, spontaneous, and chemically controlled. The negative value of  $\Delta H^\circ$  indicates that the nature of adsorption process is exothermic. This is also supported by the decrease in the uptake capacity value of the sorbent with an increase in temperature. The negative value of  $\Delta S^\circ$  shows decreased randomness at the solid/solution interfaces during the adsorption process [56–60].

### 3.5. Adsorption Isotherm

Adsorption properties and equilibrium data, commonly known as adsorption isotherms, describe how pollutants interact with adsorbent materials, so they are critical to optimizing the use of adsorbents. To optimize the design of an adsorption system to remove phenol from solutions, it is important to establish the most appropriate correlation for the equilibrium curve. An accurate mathematical description of equilibrium adsorption capacity is indispensable for reliable prediction of adsorption parameters and quantitative comparison of adsorption behavior for different adsorbent systems. Several models have been intensively used in the literature [61] to describe experimental data of adsorption isotherms. The most popular are the Langmuir, Freundlich, and Temkin models.

#### 3.5.1. Langmuir model

It suggests that pollutant removal from the aqueous phase occurs on homogeneous surfaces by monolayer sorption without interactions between sorbed molecules [62].

This adsorption model is given by:

$$\frac{Q_e}{Q_m} = \frac{K_L C_e}{1 + K_L C_e} \quad (11)$$

where  $Q_e$  is the amount of dissolved pollutant that is adsorbed on the sorbent at equilibrium ( $\text{mg g}^{-1}$ ),  $Q_m$  is the maximum adsorption capacity ( $\text{mg g}^{-1}$ ),  $C_e$  is the liquid phase concentration of the adsorbate at equilibrium ( $\text{mg L}^{-1}$ ), and  $K_L$  is the Langmuir constant related to the energy of adsorption ( $\text{L mg}^{-1}$ ). The linear form of the Langmuir isotherm equation is represented by the following equation:

$$\frac{1}{Q_e} = \frac{1}{K_L Q_m C_e} + \frac{1}{Q_m} \quad (12)$$

The maximum adsorption capacity and Langmuir constant were determined from the slope and the intercept of the plot of  $\frac{1}{Q_e}$  vs.  $\frac{1}{C_e}$  (Fig. 12).

#### 3.5.2. Freundlich isotherm

It can be expressed [63] by the following equation:

$$Q_e = K_F C_e^{\frac{1}{n}} \quad (13)$$

where  $K_F$  is a constant indicative of the adsorption capacity and  $\frac{1}{n}$  is the adsorption intensity. Eq. (13) may be linearized by taking logarithms as:

$$\ln Q_e = \ln K_F + \frac{1}{n} \ln C_e \quad (14)$$

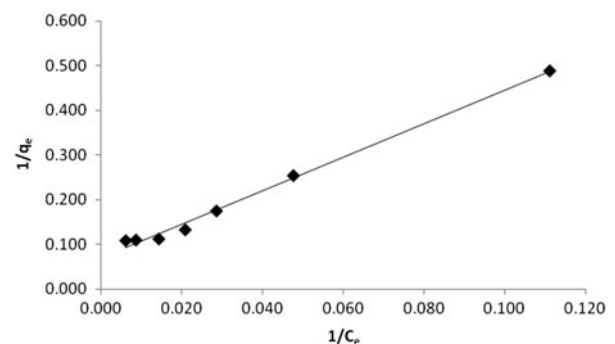


Fig. 12. Langmuir isotherm plots for the sorption of phenol onto GP (pH: 2; adsorbent dosage:  $2.1 \text{ g L}^{-1}$ ; contact time: 7 h; agitation speed: 135 rpm; Temp.:  $30^\circ\text{C}$ ).

In general, when the  $K_F$  value increases, the adsorption capacity of the sorbent for a given adsorbate increases. Furthermore, a value of the Freundlich exponent  $n$  in the range of 1–10 indicates a favorable adsorption. The linear plot of  $\ln Q_e$  vs.  $\ln C_e$  allows the estimation of  $K_F$  and  $n$  values from the intercepts and the slope of the plot (Fig. 13).

### 3.5.3. Temkin isotherm

Temkin considers the effects of some indirect adsorbate/adsorbate interactions on adsorption isotherms and suggests that, because of these interactions, the heat of adsorption of all the molecules in the layer would decrease linearly with coverage [64]. The Temkin isotherm has been used in the following form:

$$Q_e = \frac{RT}{b_T} \ln (AC_e) \tag{15}$$

$$Q_e = \frac{RT}{b_T} \ln (A) + \frac{RT}{b_T} \ln (C_e) \tag{16}$$

$B = \frac{RT}{b_T}$  is related to the heat of the adsorption process. The adsorption data can be analyzed according to the plot of  $Q_e$  vs.  $\ln C_e$ , which permits the determination of the constants A and B and  $R^2$  (Fig. 14).

The Langmuir, Freundlich, and Temkin adsorption constants are estimated from the isotherms at 30°C and their corresponding correlation coefficients are listed in Table 7. The highest regression correlation coefficient (0.998) was observed for the Langmuir model, followed by the Freundlich (0.900) and Temkin (0.936) models. This indicates that the Langmuir model was the model most suitable for describing the sorption equilibrium of phenol onto GP. This result

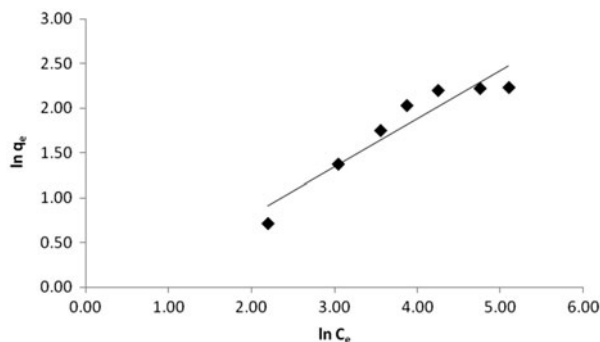


Fig. 13. Freundlich isotherm plots for the sorption of phenol onto GP (pH: 2; adsorbent dosage: 2.1 g L<sup>-1</sup>; contact time: 7 h; agitation speed: 135 rpm; Temp.: 30°C).

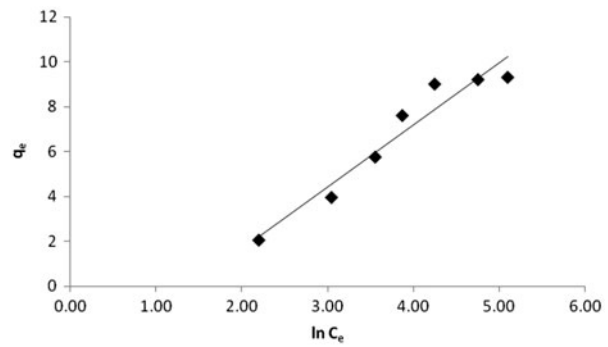


Fig. 14. Temkin isotherm plots for the sorption of phenol onto GP (pH: 2; adsorbent dosage: 2.1 g L<sup>-1</sup>; contact time: 7 h; agitation speed: 135 rpm; Temp.: 30°C).

indicates the formation of monolayer coverage of phenol molecules at the outer surface of the sorbent. The maximum adsorption capacity ( $Q_m$ ) determined from the Langmuir isotherm was calculated to be 14.49 mg g<sup>-1</sup>. If this value is relatively compared to the values reported by other studies in the literature, it is seen that this value is higher than many such values (Table 8).

### 3.6. Adsorption kinetics

To investigate the adsorption process of phenol onto GP, the frequently used kinetic models such as the linearized form of the pseudo-first-order and pseudo-second-order models given in Eqs. (17) and (18), respectively, were used to determine the mechanism of the adsorption process [74].

$$\ln (q_e - q_t) = \ln q_e - k_1 t \tag{17}$$

$$\frac{t}{q_t} = \frac{1}{k_2 q_e^2} + \frac{t}{q_e} \tag{18}$$

where  $q_e$  (mg g<sup>-1</sup>) and  $q_t$  (mg g<sup>-1</sup>) show the amount of adsorbate adsorbed on the adsorbent at equilibrium and at time  $t$ , respectively.  $k_1$  (min<sup>-1</sup>) is the pseudo-first-order rate constant.  $k_2$  (g mg<sup>-1</sup> h<sup>-1</sup>) is a second-order rate constant. The pseudo-first-order and second-order rate constants were evaluated from the linear plots of  $\ln (q_e - q_t)$  vs.  $t$ ,  $\frac{t}{q_t}$  vs.  $t$ , respectively, and are shown in Figs. 15 and 16. The correlation coefficient ( $R^2$ ) calculated from these plots was used to evaluate the applicability of these models. The correlation coefficients ( $R^2$ ), as shown in Table 9, suggest that the adsorption process follows the pseudo-second-order kinetics.

Table 6  
Thermodynamic parameters for the sorption of phenol onto GP

Initial phenol conc. ( $\text{mg L}^{-1}$ )	$\Delta G^\circ$ ( $\text{kJ mol}^{-1}$ )					$\Delta H^\circ$ ( $\text{kJ mol}^{-1}$ )	$\Delta S^\circ$ ( $\text{Jmol K}$ )
	298 (K)	303 (K)	308 (K)	313 (K)	318 (K)		
50	-3.75	-3.49	-2.42	-1.96	-1.64	-38.19	-115.31

Table 7  
Adsorption isotherm constants for phenol sorption onto GP

Isotherm	Freundlich			Langmuir			Temkin		
	$n$	$K_F$	$R^2$	$Q_m$	$K_L$	$R^2$	$A$	$B$	$R^2$
GP	1.9	0.7664	0.900	14.49	0.0183	0.998	0.2445	2.770	0.936

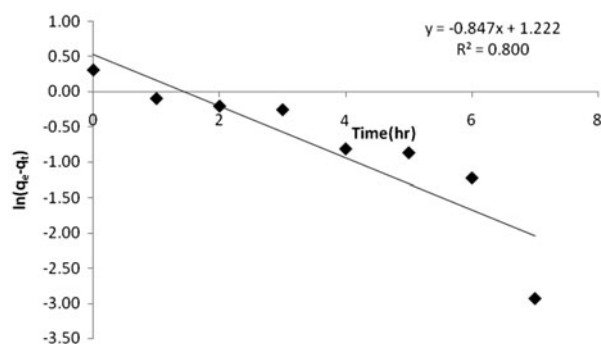


Fig. 15. Pseudo-first-order kinetic plot ( $C_0 = 50 \text{ mg L}^{-1}$ ; pH: 2; adsorbent dosage:  $2.1 \text{ g L}^{-1}$ ; contact time: 7 h; agitation speed: 135 rpm; Temp.:  $30^\circ\text{C}$ ).

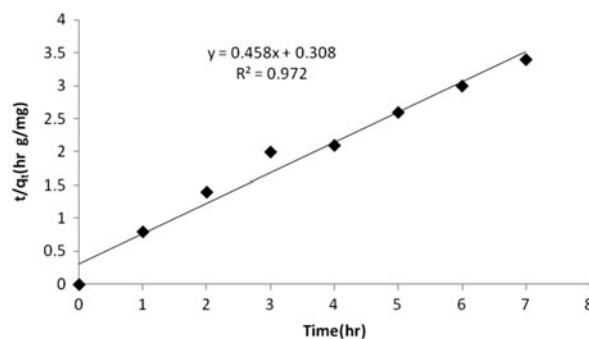


Fig. 16. Pseudo-second-order kinetic plot ( $C_0 = 50 \text{ mg L}^{-1}$ ; pH: 2; adsorbent dosage:  $2.1 \text{ g L}^{-1}$ ; contact time: 7 h; agitation speed: 135 rpm; Temp.:  $30^\circ\text{C}$ ).

Table 8  
Comparison of Langmuir adsorption capacity ( $Q_m$ ) of GP for phenol with other adsorbents in the literature

Adsorbent	Adsorption capacity ( $\text{mg g}^{-1}$ )	Reference
SDS-alumina	6.6	[65]
$\text{H}_2\text{SO}_4$ -treated <i>Aspergillus niger</i>	0.33	[66]
ZSM	7.4	[67]
Pyrolysis sewage sludge	5.6	[68]
Blast furnace sludge	7.5	[69]
Activated carbon	1.48	[70]
Hydroxyapatite nanopowers	2.98	[71]
Acid activated red mud	8.16	[72]
Vegetable sponge	4.7	[73]
Garlic peel	14.49	This work

Table 9

Kinetics constants and the correlation coefficient for different kinetic models

Adsorbent	$q_{e(\text{exp})}$ (mg/g <sup>-1</sup> )	Pseudo-first-order			Pseudo-second-order		
		$q_{e(\text{cal})}$ (mg g <sup>-1</sup> )	$k_1$ (h <sup>-1</sup> )	$R^2$	$q_{e(\text{cal})}$ (mg/g <sup>-1</sup> )	$k_2$ (g/g h <sup>-1</sup> )	$R^2$
Garlic peel	2.05	3.39	0.847	0.800	2.18	0.6837	0.978

#### 4. Conclusions

Pollutants must be removed from water to protect the environment and public health. When water is used by various sectors in society such as industries, hospitals, and households, it becomes contaminated with pollutants. If left untreated, these pollutants would negatively affect our water and environment. Wastewater treatment for the phenol in industrial and domestic effluents is very important due to its persistent toxic effects. Due to the increasing economic relevance of phenol removal, this study was conducted in an attempt to optimize the process parameters and to study the linear, square, and interactive effects of process parameters such as pH, adsorbent dosage, agitation speed, and contact time on the removal of phenol by GP. A Box–Behnken design was used to find the optimum process conditions for the removal of phenol. With the help of optimization curves, predicated maximum removal of phenol was found to be achieved at pH: 2, adsorbent dosage: 2.1 g L<sup>-1</sup>, contact time: 7 h, and agitation speed: 135 rpm. The model employed provided a good quality of predictions for these variables in terms of effective phenol degradation, and a good correlation coefficient of 0.9980 was obtained. By this model, we can predict the response for the above variables at any time. The whole process has facilitated the determination of the optimum conditions in the minimum number of experiments while allowing us to probe into possible interactions between the variables.

#### References

- [1] N. Calace, E. Nardi, B.M. Petronio, M. Pietroletti, Adsorption of phenols by papermill sludges, *Environ. Pollut.* 118 (2002) 315–319.
- [2] S. Bekkouche, S. Baup, M. Bouhelassa, S. Molina-Boisseau, C. Petrier, Competitive adsorption of phenol and heavy metal ions onto titanium dioxide (Dugussa P25), *Desalin. Water Treat.* 37 (2012) 364–372.
- [3] M.J. Ahmed, S.K. Theydan, Equilibrium isotherms, kinetics and thermodynamics studies of phenolic compounds adsorption on palm-tree fruit stones, *Ecotoxicol. Environ. Saf.* 84 (2012) 39–45.
- [4] Md. Ahmaruzzaman, Adsorption of phenolic compounds on low-cost adsorbents: A review, *Adv. Colloid Interface Sci.* 143 (2008) 48–67.
- [5] Z. Aksu, J. Yener, A comparative adsorption/biosorption study of mono-chlorinated phenols onto various sorbents, *Waste Manage.* 21 (2001) 695–702.
- [6] C. Zidi, R. Tayeb, M. Dhahbi, Extraction of phenol from aqueous solutions by means of supported liquid membrane (MLS) containing tri-n-octyl phosphine oxide (TOPO), *J. Hazard. Mater.* 194 (2011) 62–68.
- [7] M. Kobya, E. Demirbas, O. Sahin, Effect of operational parameters on the removal of phenol from aqueous solutions by electrocoagulation using Fe and Al electrodes, *Desalin. Water Treat.* 46 (2012) 366–374.
- [8] S.O.B. Boukari, F. Pellizzari, N.K.V. Leitner, Influence of persulfate ions on the removal of phenol in aqueous solution using electron beam irradiation, *J. Hazard. Mater.* 185 (2011) 844–851.
- [9] A. Bódalo, E. Gómez, A.M. Hidalgo, M. Gómez, M.D. Murcia, I. López, Nanofiltration membranes to reduce phenol concentration in wastewater, *Desalination* 245 (2009) 680–686.
- [10] J.F. García-Araya, F.J. Beltrán, P. Álvarez, F.J. Masa, Activated carbon adsorption of some phenolic compounds present in agroindustrial wastewater, *Adsorption* 9 (2003) 107–115.
- [11] A.C. Lua, Q. Jia, Adsorption of phenol by oil-palm-shell activated carbons, *Adsorption* 13 (2007) 129–137.
- [12] A. Addoun, W. Bencheikh, L. Temdrara, M. Belhachemi, A. Khelifi, Adsorption behavior of phenol on activated carbons prepared from Algerian coals, *Desalin. Water Treat.* 52 (2014) 1674–1682.
- [13] M. Belhachemi, Z. Belala, D. Lahcene, F. Addoun, Adsorption of phenol and dye from aqueous solution using chemically modified date pits activated carbons, *Desalin. Water Treat.* 7 (2009) 182–190.
- [14] A.H. Sulaymon, D.W. Abbood, A.H. Ali, A comparative adsorption/biosorption for the removal of phenol and lead onto granular activated carbon and dried anaerobic sludge, *Desalin. Water Treat.* 51 (2013) 2055–2067.
- [15] V.K. Gupta, S. Sharma, I.S. Yadav, D. Mohan, Utilization of bagasse fly ash generated in the sugar industry for the removal and recovery of phenol and *p*-nitrophenol from wastewater, *J. Chem. Technol. Biotechnol.* 71 (1998) 180–186.
- [16] M. Ahmaruzzaman, D.K. Sharma, Adsorption of phenols from wastewater. *J. Colloid Interface Sci.* 287 (2005) 14–24.
- [17] M. Otero, F. Rozada, L.F. Calvo, A.I. García, A. Morán, Elimination of organic water pollutants using adsorbents obtained from sewage sludge, *Dyes Pigm.* 57 (2003) 55–65.
- [18] H. Polat, M. Molva, M. Polat, Capacity and mechanism of phenol adsorption on lignite, *Inter. J. Miner. Process.* 79 (2006) 264–273.

- [19] E. Rubín, P. Rodríguez, R. Herrero, M.E. Sastre de Vicente, Biosorption of phenolic compounds by the brown alga *Sargassum muticum*, J. Chem. Technol. Biotechnol. 81 (2006) 1093–1099.
- [20] N.A. Darwish, K.A. Halhouli, N.M. Al-Dhoon, Adsorption of phenol from aqueous systems onto spent oil shale, Sep. Sci. Technol. 31 (1996) 705–714.
- [21] F.A. Banat, B. Al-Bashir, S. Al-Asheh, O. Hayajneh, Adsorption of phenol by bentonite, Environ. Pollut. 107 (2000) 391–398.
- [22] M. Djebbar, F. Djafri, M. Bouchekara, A. Djafri, Adsorption of phenol on natural clay, Appl. Water Sci. 2 (2012) 77–86.
- [23] M. Achak, A. Hafidi, L. Mandi, N. Ouazzani, Removal of phenolic compounds from olive mill wastewater by adsorption onto wheat bran, Desalin. Water Treat. 52 (2014) 2875–2885.
- [24] A.E. Navarro, J.C. Lazo, N.A. Cuizano, M.R. Sun-Kou, B.P. Llanos, Insights into removal of phenol from aqueous solutions by low cost adsorbents: Clays versus algae, Sep. Sci. Technol. 44 (2009) 2491–2509.
- [25] B.H. Hameed, A.A. Ahmad, Batch adsorption of methylene blue from aqueous solution by garlic peel, an agricultural waste biomass, J. Hazard. Mater. 164 (2009) 870–875.
- [26] A. Chowdhury, A. Bhowal, S. Datta, Equilibrium, Thermodynamic and kinetic studies for removal of copper (II) from aqueous solution by onion and garlic skin, Water 4 (2012) 37–51.
- [27] W. Liu, Y. Liu, Y. Tao, Y. Yu, H. Jiang, H. Lian, Comparative study of adsorption of Pb(II) on native garlic peel and mercerized garlic peel, Environ. Sci. Pollut. Res. Int. 21 (2014) 2054–2063.
- [28] S. Liang, X. Guo, Q. Tian, Adsorption of Pb<sup>2+</sup>, Cu<sup>2+</sup> and Ni<sup>2+</sup> from aqueous solutions by novel garlic peel adsorbent, Desalin. Water Treat. 51 (2013) 7166–7171.
- [29] M. Ichikawa, K. Ryu, J. Yoshida, N. Ide, Y. Kodera, T. Sasaoka, R.T. Rosen, Identification of six phenylpropanoids from garlic skin as major antioxidants, J. Agric. Food Chem. 51 (2003) 7313–7317.
- [30] M. Rajasimman, R. Sangeetha, P. Karthik, Statistical optimization of process parameters for the extraction of chromium (VI) from pharmaceutical wastewater by emulsion liquid membrane, Chem. Eng. J. 150 (2009) 275–279.
- [31] J. Si, B. Cui, Dye congo red adsorptive decolorization by adsorbents obtained from trametes pubescens pellets, Desalin. Water Treat. 51 (2013) 7088–7100.
- [32] S. Dutta, Optimization of Reactive Black 5 removal by adsorption process using Box-Behnken design, Desalin. Water Treat. 51 (2013) 7631–7638.
- [33] C.Y. Su, W.G. Li, X.Z. Liu, L. Zhang, Adsorption property of direct red brown onto acid-thermal-modified sepiolite and optimization of adsorption conditions using Box-Behnken response surface methodology, Desalin. Water Treat. 52 (2014) 880–888.
- [34] V. Ponnusami, V. Gunasekar, S.N. Srivastava, Kinetics of methylene blue removal from aqueous solution using gulmohar (*Delonix regia*) plant leaf powder: Multivariate regression analysis, J. Hazard. Mater. 169 (2009) 119–127.
- [35] A. Gundogdu, C. Duran, H. Basri Senturk, M. Soylak, D. Ozdes, H. Serencam, M. Imamoglu, Adsorption of phenol from aqueous solution on a low-cost activated carbon produced from tea industry waste: Equilibrium, kinetic, and thermodynamic study, J. Chem. Eng. Data 57 (2012) 2733–2743.
- [36] B. Subramanyam, A. Das, Study of the adsorption of phenol by two soils based on kinetic and isotherm modeling analyses, Desalination 249 (2009) 914–921.
- [37] A. Mittal, D. Kaur, A. Malviya, J. Mittal, V.K. Gupta, Adsorption studies on the removal of coloring agent phenol red from wastewater using waste materials as adsorbents, J. Colloid Interface Sci. 337 (2009) 345–354.
- [38] S.H. Lin, R.S. Juang, Adsorption of phenol and its derivatives from water using synthetic resins and low-cost natural adsorbents: A review, J. Environ. Manage. 90 (2009) 1336–1349.
- [39] A. Dąbrowski, P. Podkościelny, Z. Hubicki, M. Barczak, Adsorption of phenolic compounds by activated carbon—a critical review, Chemosphere 58 (2005) 1049–1070.
- [40] R.K. Xu, S.C. Xiao, J.H. Yuan, A.Z. Zhao, Adsorption of methyl violet from aqueous solutions by the biochars derived from crop residues, Bioresour. Technol. 102 (2011) 10293–10298.
- [41] Y. Li, Q. Du, T. Liu, X. Peng, J. Wang, J. Sun, Y. Wang, S. Wu, Z. Wang, Y. Xia, L. Xia, Comparative study of methylene blue dye adsorption onto activated carbon, graphene oxide, and carbon nanotubes, Chem. Eng. Res. Des. 91 (2013) 361–368.
- [42] Z. Wu, H. Joo, K. Lee, Kinetics and thermodynamics of the organic dye adsorption on the mesoporous hybrid xerogel, Chem. Eng. J. 112 (2005) 227–236.
- [43] M. Manshour, H. Daraei, A.R. Yazdanbakhsh, A feasible study on the application of raw ostrich feather, feather treated with H<sub>2</sub>O<sub>2</sub> and feather ash for removal of phenol from aqueous solution, Desalin. Water Treat. 41 (2012) 179–185.
- [44] G. Busca, S. Berardinelli, C. Resini, L. Arrighi, Technologies for the removal of phenol from fluid streams: A short review of recent developments, J. Hazard. Mater. 160 (2008) 265–288.
- [45] F.A. Abu Al-Rub, J. Hamdi, N. Hamdi, H. Allaboun, M. Al Zarooni, M. Al-Sharyani, Adsorption of phenol on different activated carbons prepared from date pits, Sep. Sci. Technol. 46 (2010) 300–308.
- [46] C.Y. Cao, L.K. Meng, Y.H. Zhao, Adsorption of phenol from wastewater by organo-bentonite, Desalin. Water Treat. 52 (2014) 3504–3509.
- [47] M. Ahmaruzzaman, Role of fly ash in the removal of organic pollutants from wastewater, Energy Fuels 23 (2009) 1494–1511.
- [48] M.A. Hararah, K.A. Ibrahim, A.H. Al-Muhtaseb, R.I. Yousef, A. Abu-Surrah, A. Qatatsheh, Removal of phenol from aqueous solutions by adsorption onto polymeric adsorbents, J. Appl. Polym. Sci. 117 (2010) 1908–1913.
- [49] M.T. Yagub, T.K. Sen, H.M. Ang, Equilibrium, kinetics, and thermodynamics of methylene blue adsorption by pine tree leaves, Water Air Soil Pollut. 223 (2012) 5267–5282.
- [50] S.M. Mane, A.K. Vanjara, M.R. Sawant, Removal of phenol from wastewater using date seed carbon, J. Chin. Chem. Soc. 52 (2005) 1117–1122.
- [51] D. Park, Y.S. Yun, J.M. Park, The past, present, and future trends of biosorption, Biotechnol. Bioprocess Eng. 15 (2010) 86–102.

- [52] R. Rajeshkannan, M. Rajasimman, N. Rajamohan, Optimization, equilibrium and kinetics studies on sorption of Acid Blue 9 using brown marine algae *Turbinaria conoides*, *Biodegradation* 21 (2010) 713–727.
- [53] A.T. Mohd Din, B.H. Hameed, A.L. Ahmad, Batch adsorption of phenol onto physiochemical-activated coconut shell, *J. Hazard. Mater.* 161 (2009) 1522–1529.
- [54] H.B. Senturk, D. Ozdes, A. Gundogdu, C. Duran, M. Soylak, Removal of phenol from aqueous solutions by adsorption onto organomodified Tirebolu bentonite: Equilibrium, kinetic and thermodynamic study, *J. Hazard. Mater.* 172 (2009) 353–362.
- [55] A. Kuleyin, Removal of phenol and 4-chlorophenol by surfactant-modified natural zeolite, *J. Hazard. Mater.* 144 (2007) 307–315.
- [56] Z. Ghasemi, A. Seif, T.S. Ahmadi, B. Zargar, F. Rashidi, G.M. Rouzbahani, Thermodynamic and kinetic studies for the adsorption of Hg(II) by nano-TiO<sub>2</sub> from aqueous solution, *Adv. Powder Technol.* 23 (2012) 148–156.
- [57] M. Ahmaruzzaman, S. Laxmi Gayatri, Activated neem leaf: A novel adsorbent for the removal of phenol, 4-nitrophenol, and 4-chlorophenol from aqueous solution, *J. Chem. Eng. Data* 56 (2011) 3004–3016.
- [58] C. Hua, R. Zhang, L. Li, X. Zheng, Adsorption of phenol from aqueous solutions using activated carbon prepared from crofton weed, *Desalin. Water Treat.* 37 (2012) 230–237.
- [59] P. Senthil Kumar, K. Ramakrishnan, S. Dinesh Kirupha, S. Sivanesan, Thermodynamic, kinetic, and equilibrium studies on phenol removal by use of cashew nut shell, *Can. J. Chem. Eng.* 89 (2011) 284–291.
- [60] Q.S. Liu, T. Zheng, P. Wang, J.P. Jiang, N. Li, Adsorption isotherm, kinetic and mechanism studies of some substituted phenols on activated carbon fibers, *Chem. Eng. J.* 157 (2010) 348–356.
- [61] M.A. Hossain, H.H. Ngo, W.S. Guo, T.V. Nguyen, Palm oil fruit shells as biosorbent for copper removal from water and wastewater: Experiments and sorption models, *Bioresour. Technol.* 113 (2012) 97–101.
- [62] I. Langmuir, The adsorption of gases on plane surfaces of glass, mica and platinum, *J. Am. Chem. Soc.* 40 (1918) 1361–1403.
- [63] K. Vijayaraghavan, T.V.N. Padmesh, K. Palanivelu, M. Velan, Biosorption of nickel (II) ions onto *Sargassum wightii*. Application of two-parameter and three-parameter isotherm models. *J. Hazard. Mater.* 133 (2006) 304–308.
- [64] O. Hamdaoui, E. Naffrechoux, Modeling of adsorption isotherms of phenol and chlorophenols onto granular activated carbon: Part I. Two-parameter models and equations allowing determination of thermodynamic parameters, *J. Hazard. Mater.* 147 (2007) 381–394.
- [65] A. Adak, A. Pal, M. Bandyopadhyay, Removal of phenol from water environment by surfactant-modified alumina through adsolubilization, *Colloids Surf., A* 277 (2006) 63–68.
- [66] J.R. Rao, T. Viraraghavan, Biosorption of phenol from an aqueous solution by *Aspergillus niger* biomass, *Bioresour. Technol.* 85 (2002) 165–171.
- [67] M. Ghiaci, A. Abbaspur, R. Kia, F. Seyedejn-Azad, Equilibrium isotherm studies for the sorption of benzene, toluene, and phenol onto organo-zeolites and as-synthesized MCM-41, *Sep. Purif. Technol.* 40 (2004) 217–229.
- [68] S. Rio, C. Faur-Brasquet, L. Le Coq, P. Le Cloirec, Structure characterization and adsorption properties of pyrolyzed sewage sludge, *Environ. Sci. Technol.* 39 (2005) 4249–4257.
- [69] A.K. Jain, V.K. Gupta, S. Jain, Removal of chlorophenols using industrial wastes, *Environ. Sci. Technol.* 38 (2004) 1195–1200.
- [70] I. Vazquez, J. Rodriguez-Iglesias, E. Maranon, L. Castrillon, M. Alvarez, Removal of residual phenols from coke wastewater by adsorption, *J. Hazard. Mater.* 147 (2007) 395–400.
- [71] K. Lin, J. Pan, Y. Chen, R. Cheng, X. Xu, Study the adsorption of phenol from aqueous solution on hydroxyapatite nanopowders, *J. Hazard. Mater.* 161 (2009) 231–240.
- [72] A. Tor, Y. Cengeloglu, M. Ersoz, Increasing the phenol adsorption capacity of neutralized red mud by application of acid activation procedure, *Desalination* 242 (2009) 19–28.
- [73] H. Cherifi, S. Hanini, F. Bentahar, Adsorption of phenol from wastewater using vegetal cords as a new adsorbent, *Desalination* 244 (2009) 177–187.
- [74] N.S. Kumar, M. Suguna, M.V. Subbaiah, A.S. Reddy, N.P. Kumar, A. Krishnaiah, Adsorption of phenolic compounds from aqueous solutions onto chitosan-coated perlite beads as biosorbent, *Ind. Eng. Chem. Res.* 49 (2010) 9238–9247.